Front. Optoelectron. 2016, 9(4): 535–543
DOI 10.1007/s12200-016-0541-3

REVIEW ARTICLE

A tutorial introduction to graphene-microfiber waveguide and its applications

Xiaoying HE (✉), Min XU, Xiangchao ZHANG, Hao ZHANG

Shanghai Engineering Research Center of Ultra-Precision Optical Manufacturing, Department of Optical Science and Engineering, Fudan University, Shanghai 200433, China

Abstract Graphene-microfiber with the advantage of graphene material and the microfiber has been hailed as a wonderful waveguide in optics. A tutorial introduction to the graphene-microfiber (GMF) waveguides including the effect of graphene on waveguide, fabrication and applications has been presented. Here, we reviewed recent progress in the graphene waveguides from mode-locking and *Q*-switching in fiber laser to gas sensing and optical modulation. A brief outlook for opportunities and challenges of GMF in the future has been presented. With the novel nanotechnology emerging, GMF could offer new possibilities for future-optic circuits, systems and networks.

Keywords graphene, microfiber, optical mode locking, optical sensor

1 Introduction

Two dimensional (2D) hexagonal lattice forms of carbon, graphene, have attracted significant attentions because it exhibits a variety of exceptional photonic and electronic properties [1–3]. Graphene offers a high intrinsic mobility of 200000 $cm^2/(v \cdot s)$ [4,5], and large Young's modulus of ~1.0 TPa, extraordinary thermal conductivity as well as gate-variable optical conductivity [6]. These features make graphene ideal for use in the field of nano-electronics and sensors. Because of its unique electronic structure and linear dispersion, a monolayer graphene shows a constant absorption per unit mass of the material (2.3%) from the ultraviolet (UV) to the infrared [7,8]. Compared to many other optical materials [9–11], graphene also has ultrafast carrier dynamics response [12–15] over an ultra-broadband spectral range. Such ultrafast carrier dynamics and the Pauli blocking effect enable graphene to exhibit many remarkable nonlinear optical properties [15,16] such as saturable absorptions, high Kerr nonlinearity (nonlinear refractive index change), two-photon absorption, four-wave mixing (FWM) [17,18], and so on. As a atomically thin film, it is flexible to be incorporated into other photoelectric materials [19–22], such as silicon, silica, semiconductor materials. Recently, a number of graphene photonic devices [19–23], e.g., polarizers [22], photo-receivers [19,20], modulator [21], and etc., have been reported for wide applications to photonic integrated circuits, optical communication, and sensing.

Microfiber as one dimensional (1D) micro/nano scale waveguide with tight optical confinement and strong evanescent fields [24–27] can effectively collect and launch the evanescent light to excite the evanescent coupling between a microfiber and other waveguide. In the graphene-microfiber (GMF) waveguide, the large evanescent light enables strong or rapid near-field interaction between the guide light and the graphene to excite the third-order nonlinearity of the graphene, e.g., nonlinear saturable absorption and Kerr nonlinearity [16], thus leading to the optical modulation [28,29], sensing element [30–33], and saturable absorber [34–47] for many potential application. Here we review the recent progress about the GMF waveguide regarding their waveguide structure, optical properties, fabrication, and sensing and laser applications. We will start from the fundamentals of the GMF waveguide, and then move to the applications of such waveguide. Finally, a brief outlook for opportunities and challenges of GMF in the future has been presented.

2 Fundamentals of GMF waveguide

2.1 Structure and fabrication

To date, the GMF waveguides have three kinds of structures, as shown in Fig. 1. The first structure

Received July 7, 2015; accepted November 18, 2015

E-mail: xiaoyinghe@fudan.edu.cn

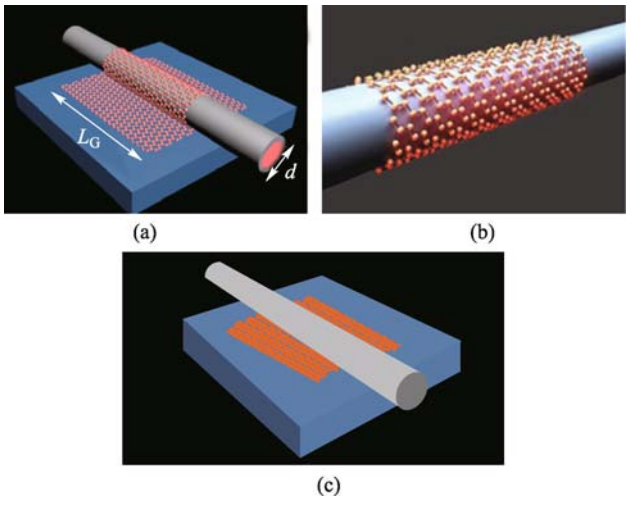

Fig. 1 Schematic diagram of GMF waveguide [29–31]. L_G is the length of graphene, d is the microfiber diameter

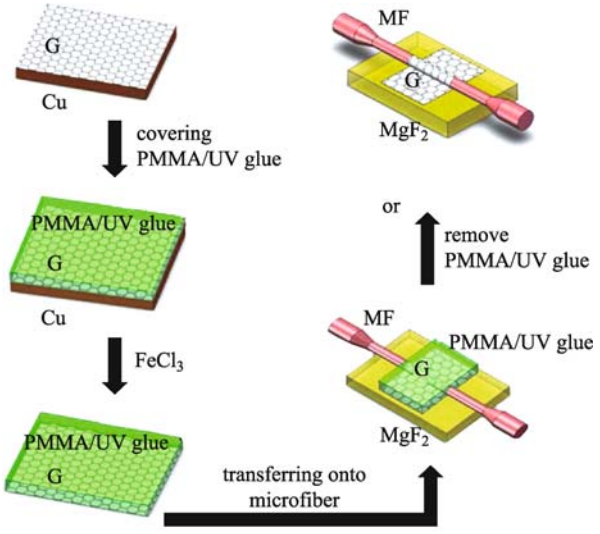

Fig. 2 Fabrication process of GMF waveguide in Fig. 1(a) [31]. G: graphene

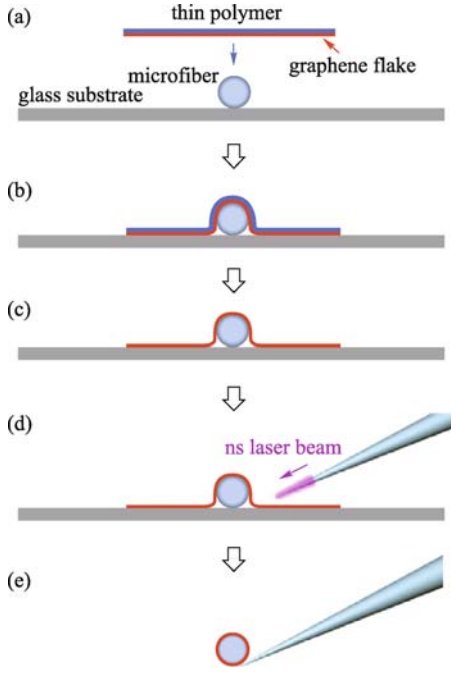

Fig. 3 Fabrication process of GMF waveguide in Fig. 1(b) [29]

configuration of the GMF waveguide is shown in Fig. 1(a), where the graphene films is tightly covered on the microfiber onto the MgF_2 substrate. Figure 1(b) shows the graphene film is wrapped around the microfiber, which presents the second structure configuration. The last in Fig. 1(c) shows the microfiber tightly attached on the graphene film, which is deposited on an MgF_2 substrate.

To our knowledge, the microfiber in the GMF waveguide is fabricated by flame-heated taper-drawing technology [24] with the diameter down to micro/nano-scale, because this technique could reduce the propagation loss and realize the tapering profile optimization and cross-section geometric control.

Here, we demonstrate two kinds of GMF waveguides fabrication process (Figs. 1(a) and 1(b)) in this paper, as shown in Figs. 2 [31] and 3 [29]. For the first structure, the graphene film is grown on the surface of Cu or Ni by chemical vapor deposition (CVD) method, and then the low refractive index polymethyl methacrylate (PMMA) or UV glue is spin-coated on the graphene film surface, and is then cured to form a polymer/graphene/metal sandwich structure. To remove the metal layer, it can be soaked into the $FeCl_3$ solution with a long time. Subsequently, the polymer-supported graphene washes in deionized (DI) water several times and covered on the microfiber/MgF_2. The PMMA or UV glue could be removed by acetone for our consideration. Finally, we put it in a box to dry at room temperature for 12 h. The GMF waveguide with the third structure has the similar fabrication process. One of fabrication methods about the second structure in Fig. 1 (b) is presented in Fig. 3. The PMMA is spin-coated on the surface of the graphene/Cu or graphene/Ni/SiO_2, and then we use the $FeCl_3$ solution to remove the metal layer. An obtained PMMA/graphene film is cleaned by DI water and is then draped over a microfiber (Fig. 3(b)). An acetone solution at room temperature is then used to remove the PMMA, holding only graphene on the microfiber (Fig. 3 (c)). A ns laser beam through a typed-fiber tip is employed to cut the graphene. When we lifted the microfiber, the graphene film was wrapped over the microfiber to from a GMF waveguide (in Fig. 3(e)).

2.2 Effect of graphene on the waveguide

To analyze the effect of graphene on the dispersion of the waveguide, the dynamical conductivity σ_g of graphene

should be considered in the Maxwell's equations. The conductivity of graphene is related with radian frequency (ω), chemical potential (μ_c), the relaxation time (τ), and temperature (T). Here, it can be calculated from the Kubo formula:

$$\begin{aligned}&(\omega,\mu_c,\Gamma,T)\\&=\frac{je^2(\omega-j\tau^{-1})}{\pi\hbar}\frac{1}{(\omega-j\tau^{-1})^2}\\&\times\int_0^\infty\varepsilon\left(\frac{\partial f_d(\varepsilon)}{\partial\varepsilon}-\frac{\partial f_d(-\varepsilon)}{\partial\varepsilon}\right)d\varepsilon\\&-\frac{je^2(\omega-j\tau^{-1})}{\pi\hbar}\int_0^\infty\frac{f_d(-\varepsilon)-f_d(\varepsilon)}{(\omega-j2\Gamma)^2-4(\varepsilon/\hbar)^2}d\varepsilon,\end{aligned}\quad(1)$$

where e is the charge of an electron, $\hbar=h/2\pi$ is the reduced Planck's constant, $f_d(\varepsilon)=[e^{(\varepsilon-\mu_c)/(k_BT)}+1]^{-1}$ is the Fermi-Dirac distribution, and k_B is Boltzmann's constant. The first term in Eq. (1) is evaluated as the intraband conductivity, and the second is due to the interband contribution. The permittivity of the graphene is related with the conductivity as $\varepsilon_g=\varepsilon_0-\sigma_{g,i}/(\omega d)+j\sigma_{g,r}/(\omega d)$ [46], where $\sigma_{g,i}$ and $\sigma_{g,r}$ are the imaginary and real part of the conductivity of graphene σ_g, and d is the thickness of the graphene film, and ω is the light's angular frequency. Figure 4 shows the real and imaginary parts of the conductivity and the permittivity of an infinite graphene sheet at wavelength 1550 nm. From Fig. 4, the ε-near zero point is at the chemical potential μ_{c0} = 0.5 eV, where the imaginary part of epsilon shows a constant value. When the chemical potential is low to μ_{c0}, the real and imaginary parts of the permittivity of graphene have positive sign, that make it behaves like a dielectric material. When $\mu_c>0.5$ eV, Re(ε) becomes negative and Im(ε) is approaching zero, so that the graphene shows the behavior of metallic material. Thus, the material property of graphene is easily controlled by the chemical potential (μ_c) from dielectric to metallic behavior. In intrinsic graphene, the Fermi energy is near to zero, thus μ_c is equal to 0.0002 eV. By applying $\omega^2\mu_0\varepsilon=n^2k_0^2$, the refractive indexes about the intrinsic monolayer graphene is calculated in Fig. 5 as a function of the wavelength from 500 to 2000 nm. The real and imaginary parts of the graphene refractive index is respectively changed from 1.8 to 3.38, and 1.6 to 3.2. That means the refractive index would increase with the increase of the wavelength.

To analyze the effect of the graphene on the GMF waveguide, we choose the model in Fig. 1(b) as a case, which has been displayed in Fig. 6. The microfiber mainly depends on the strong evanescent field to interact with graphene sheet, so that the graphene sheet warped over the microfiber could affect the electric field distribution,

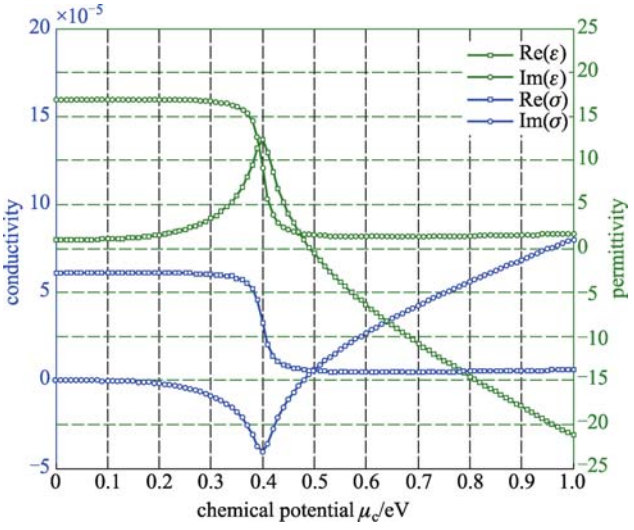

Fig. 4 Real and imaginary parts of the conductivity and the permittivity of infinite graphene sheet at wavelength 1550 nm

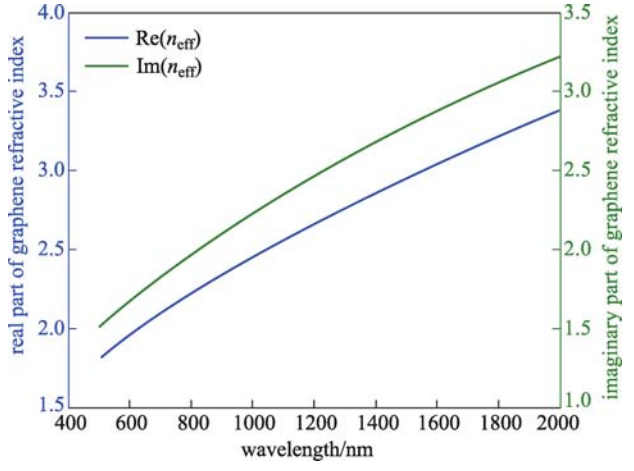

Fig. 5 Real and imaginary parts of the refractive index of the intrinsic monolayer graphene sheet vs. the wavelength

effective refractive index, optical confinement, and so on. Figures 6 (a) and 6(b) are the cross-sectional profiles of the microfiber and the graphene warped over the microfiber, respectively. The index of the microfiber is 1.47, and the simulation index of graphene comes from Fig. 5. The simulation transmission wavelength in the microfiber and GMF waveguide is at 1550 nm. Figures 6(c) and 6(d) presents the electric field distribution of the fundamental HE_{11} mode of the microfiber and the GMF waveguide, respectively. Figures 6(e) and 6(f) shows the 1D power distribution of electric filed in the microfiber and the GMF waveguide, respectively. It can be observed that graphene wrapped over the microfiber could enhance the evanescent field in the microfiber, thus leading to more light from the guided light to interact with the graphene. These simulated

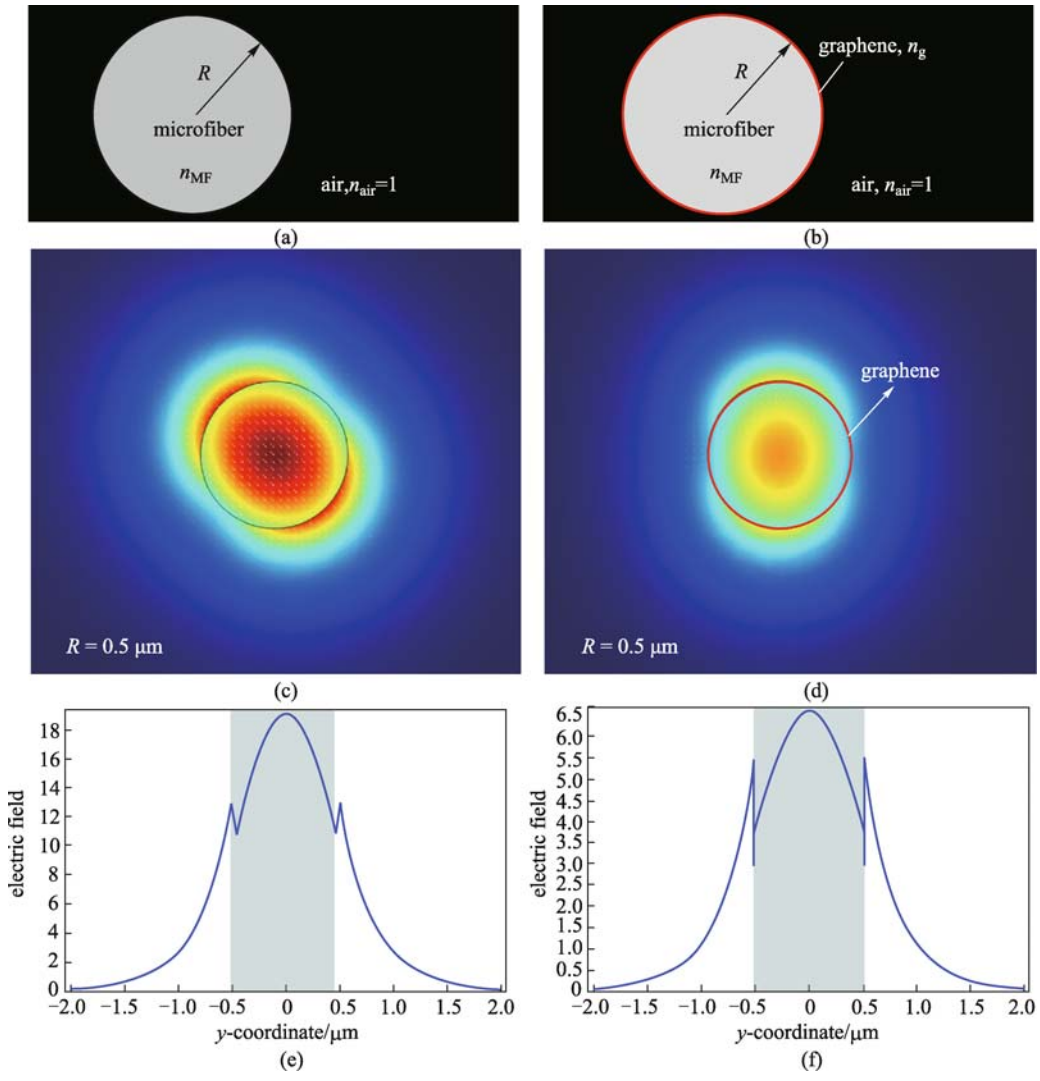

Fig. 6 (a) and (b) Cross-sectional views of microfiber and GMF waveguide; (c) and (d) electric field distribution in the cross section of microfiber and GMF waveguide; (e) and (f) field distribution along the *y*-coordinate direction in microfiber and GMF waveguide

results in Figs. 6(e) and 6(f) also show the optical field in the microfiber has more tight confinement than that of the GMF waveguide.

3 Application of GMF waveguide

Inspired by the great curiosity, the research on the optical GMFs has attracted more and more attentions. The research on the GMFs mainly in the last two or three years has brought massive opportunities in renewing the fiber optic technology on micro/nano scale. In short, these recent advances are categorized into three areas: lasers, sensors, signals processing.

3.1 Laser applications

Graphene is first found to have saturable absorption properties in 2009, and is applied in fiber laser for mode-locking by Bao et al. [48] and Sun et al. [34]. In 2012, He et al. used the reduced graphene oxides on the microfiber for passive mode-locking in Erbium-doped fiber laser to generate a wide-band doublet pulses [35]. Subsequently, more and more papers were reported by using the GMF for *Q*-switching and mode-locking. In 2013, Sheng et al. employed the GMF in Erbium doped fiber laser to operate at switchable working states from stable *Q*-switching to stable mode-locking by tuning the polarization states in cavity [36,37]. As shown in Fig. 7, by tuning the polarization of the light propagated in the GMF, soliton pulses with tunable pulse-width were obtained from ~ 522 to ~459 fs with 3 dB spectral bandwidth from ~2.4 to 10 nm [35], and pulse-width-tuned dissipative pulses were obtained from ~9.24 to ~2.32 ps with 3 dB spectral bandwidth from ~6.03 to 26.32 nm [38]. Figures 7(a) and 7(b) are the experimental setups respectively in Refs. [38] and [39]. The GMF not only acts as a saturable absorber, but also forms an artificial birefringent filter in fiber laser

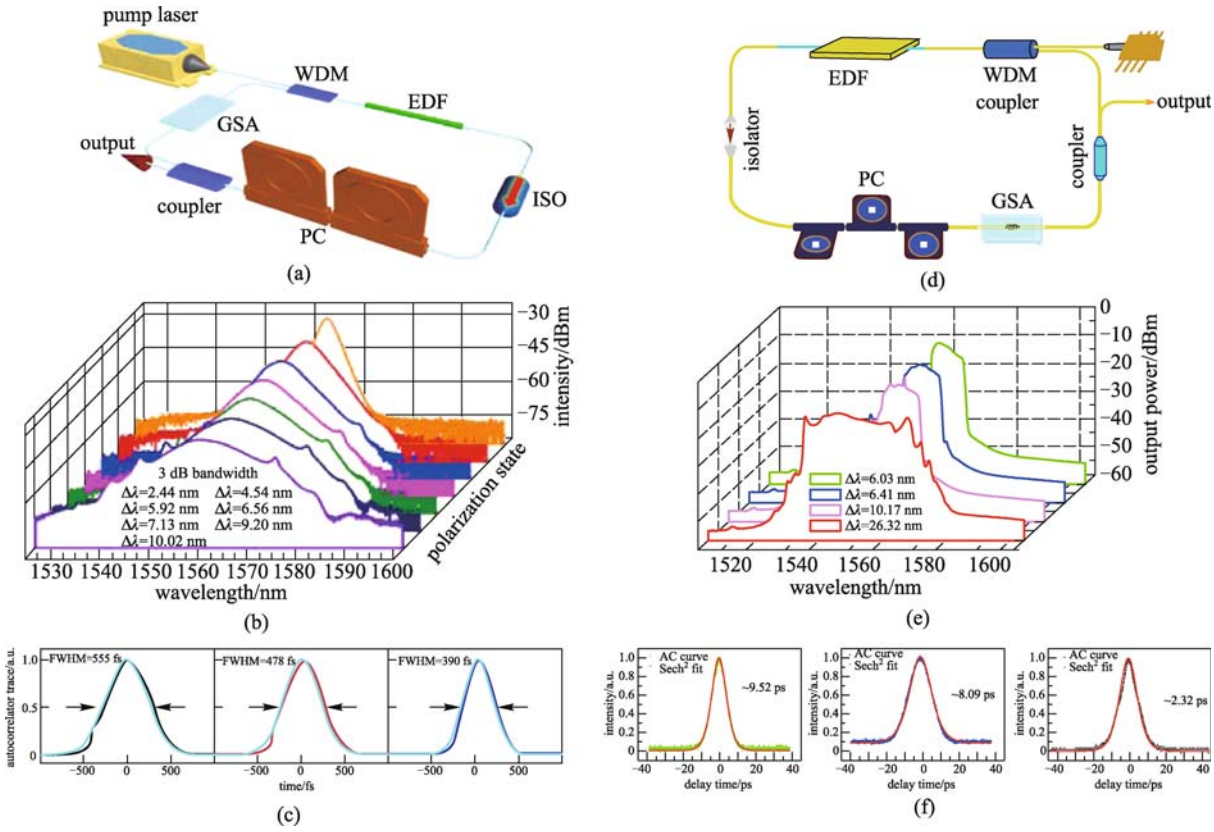

Fig. 7 Pulse-width-tuned pulses generated by GMF passive mode-locking [38,39]. GSA: graphene saturable absorber, PC: polarized controller, WDM: wavelength division multiplex, EDF: Erbium-doped fiber

for multi-wavelengths continuous-wave mode-locking operation [40]. A versatile soliton has been obtained in fiber laser by the highly nonlinear GMF mode-locking [41].

Due to the line dispersion, graphene as promising material has wide-band saturable absorption, thus the GMF as saturable absorber is utilized in the Yb-doped fiber laser system [42], and Tm^{3+}-doped fiber laser system [43]. Due to the broadband advantage of graphene, the GMF with various modulation depth by employing the effects of cross absorption modulation is utilized in fiber laser for realizing the pulse-width tuning [44] and actively *Q*-swithing [45].

Beside the mode-locking by using the GMF, the passive *Q*-switching phenomenon generated by GMF in fiber laser had also been observed [36,37,45]. Ahmad et al. reported a dual wavelength passive *Q*-switching in Erbium-doped fiber laser by using the GMF in a nonlinear loop mirror [46], and Qi et al. presented a high-repetition-rate pulse generation obtained by a fiber laser based on a graphene-deposited microfiber and a Fabry-Perot filter [47].

3.2 Sensing applications

Graphene as a smart 2D material with large surface area for molecular absorption, and conductivity tuning via chemical doping has a potential application in optical biochemical sensing application. Recently, there are several reports on sensor applications of the GMF. The GMF for volatile chemical gas sensing [30] was reported by Wu et al., where two tapered fibers covered with graphene have an unsteady structure to limit its sensitivity. When the gas molecules go through the sensor, the gas molecules had been absorbed by van der Walls force of graphene, which would alter the initial hexagonal structure of graphene to change the spatial distribution of electrical carriers [49]. Subsequently, graphene coated on the microfiber-based Bragg grating (MFBG) has been developed from the GMF waveguide for fiber-optical gas sensor by Wu et al. [33]. Figure 8 shows the GMF gas sensors reported in the paper [33]. Compared with the MFBG sensor, such graphene-coated MFBG has ~10 times higher sensitivities around ~0.2 and ~0.5 ppm[1)] for NH_3 and xylene gas, respectively, than that of the MFBG. Meanwhile, the GMF is utilized in Mach-Zehnder interferometric for gas sensor for NH_3 gas sensor [31,32]. Yan et al. reported an optical electrical current sensor utilizing a GMF-integrated coil resonator with a high sensitivity of 67.297 μm/A^2 [50]. Those works could open a window for the development of GMF-based

1) 1 ppm = 1×10^{-6}

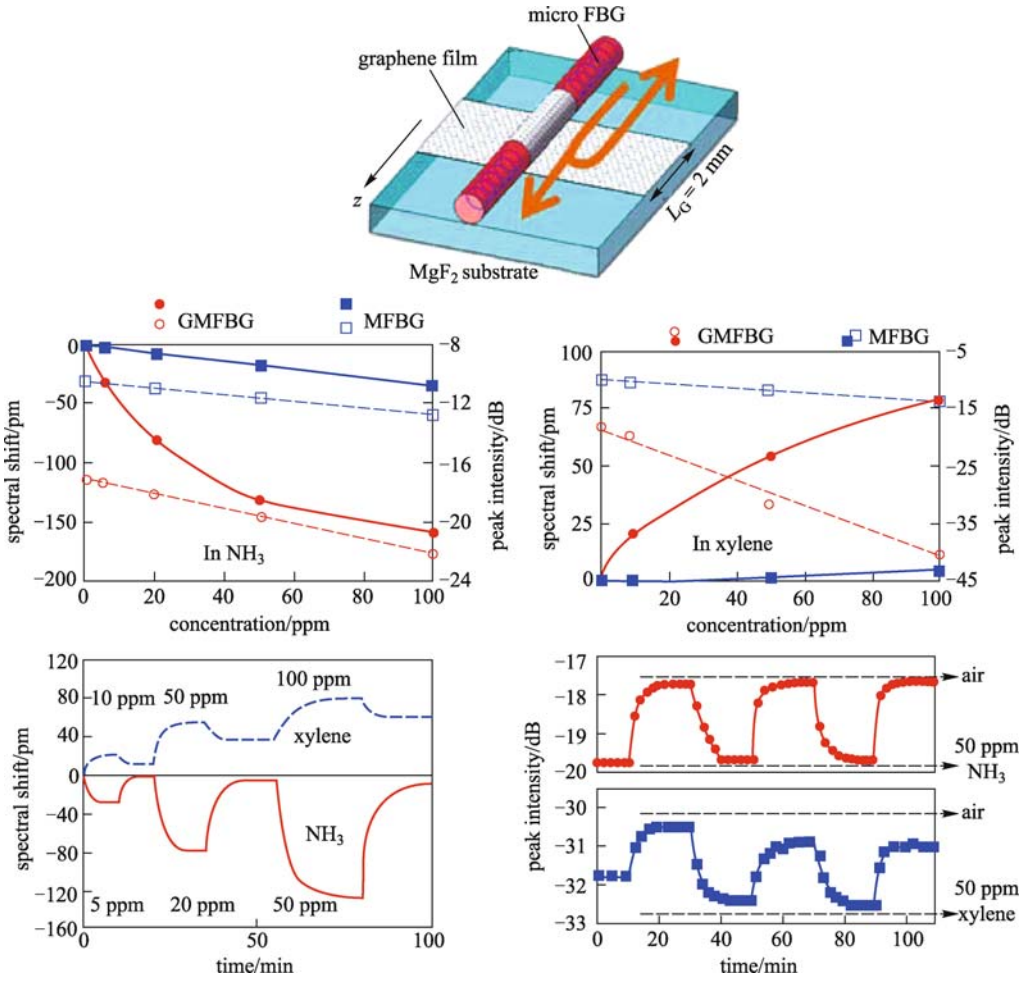

Fig. 8 Experimental results of GMF gas sensors [33]

gas sensors with high sensitivity, low cost, and small footprint.

3.3 Other photonic devices

The GMF is not only used for pulse generation or gas sensors in fiber system, but also can realizing the signal processing, such as optical signal modulation [28,29], optical polarization selection [51], broadband photo detection [52] and microbubble generation depended on photo-thermal phenomenon [53]. Recently, the GMF was demonstrated as broadband all-optical modulator with a modulation rate of 1 MHz [28] or 200 GHz [29], due to the cross absorption modulation. Especially, this high speed all-optical modulator can be compatible with current high speed fiber communication and open the gate to the ultrafast signal processing on fiber. We had made a asymmetry microfiber-graphene configuration work at small size to perform a polarization-dependent property [51], which had a potential application for polarization selection. Subsequently, a broadband photodetection can also be realized by a microfiber-garphene device owing to the interaction between the graphene film and the evanescent field leaked from the microfiber, which exhibits a high photoresponse from 1500 to 1600 nm [52]. Consequently, Xing et al. utilized the photo-thermal effect of graphene oxide nanosheets on the microfiber to produce microbubbles, which has prospective applications in sensing, microfluidics, virus detection and other biochip techniques [53]. It is generally known that graphene surface plasmons have excellent field confinement and could be restricted on graphene surfaces. The graphene-coated nanowire probe with circular aperture could offer larger field enhancements on the surface of the probe by graphene surface plasmons than other plasmon-based probe [54].

4 Conclusions

As a novel fiber-based device, the GMF, which comes from the seamless integration of fiber optics and graphene photonics, has been introduced in this paper. So far, it not only had been used as saturable absorber in fiber laser for mode-locking and Q-switching, but also had opened up new opportunities in gas sensors, optical signal processing,

microfluidics [51], bio-sensors, and so on. However, all these applications are based on the nonlinear saturable absorption and the conductivity tuning via chemical doping properties of graphene and the strong evanescent field of the microfiber. Except discussed above, graphene has superior features, such as larger nonlinear Kerr effect, FWM, two-photonic absorption, electrically tuning the Fermi level, surface plasmons like metal, and so on. In the future, these features should be considered in the GMF to offer new potential applications in every domains, e.g., super-resolution imaging, sensing, signal processing in optical fiber communication, microfluidics. With the fast growing of nanotechnology, there are many challenges to be addressed to fabricate the GMF with low loss, better protection technology, length increasing, which may offer new possibilities for future-optic circuits, systems and networks.

Acknowledgements This work was supported by the National Natural Science Foundation of China (Grant No. 61205132), Research Fund for the Doctoral Program of Higher Education of China (No. 20120071120023), the Fundamental Research Funds for the Central University (Nos. GKH1232000/007, 20520133249 and 20520131128) and Funds for Shanghai ultra-precision optical manufacturing engineering technology research center (No. 11DZ2282200).

References

1. Bonaccorso F, Sun Z, Hasan T, Ferrari A C. Graphene photonics and optoelectronics. Nature Photonics, 2010, 4(9): 611–622
2. Avouris P. Graphene: electronic and photonic properties and devices. Nano Letters, 2010, 10(11): 4285–4294
3. Novoselov K S, Geim A K, Morozov S V, Jiang D, Katsnelson M I, Grigorieva I V, Dubonos S V, Firsov A A. Two-dimensional gas of massless Dirac fermions in graphene. Nature, 2005, 438(7065): 197–200
4. Bolotin K I, Sikes K J, Jiang Z, Klima M, Fudenberg G, Hone J, Kim P, Stormer H L. Ultrahigh electron mobility in suspended graphene. Solid State Communications, 2008, 146(9-10): 351–355
5. Morozov S V, Novoselov K S, Katsnelson M I, Schedin F, Elias D C, Jaszczak J A, Geim A K. Giant intrinsic carrier mobilities in graphene and its bilayer. Physical Review Letters, 2008, 100(1): 016602-1–016602-4
6. Wang F, Zhang Y, Tian C, Girit C, Zettl A, Crommie M, Shen Y R. Gate-variable optical transitions in graphene. Science, 2008, 320 (5873): 206–209
7. Nair R R, Blake P, Grigorenko A N, Novoselov K S, Booth T J, Stauber T, Peres N M R, Geim A K. Fine structure constant defines visual transparency of graphene. Science, 2008, 320(5881): 1308-1–1308-7
8. Casiraghi C, Hartschuh A, Lidorikis E, Qian H, Harutyunyan H, Gokus T, Novoselov K S, Ferrari A C. Rayleigh imaging of graphene and graphene layers. Nano Letters, 2007, 7(9): 2711–2717
9. Almeida V R, Barrios C A, Panepucci R R, Lipson M. All-optical control of light on a silicon chip. Nature, 2004, 431(7012): 1081–1084
10. Pacifici D, Lezec H J, Atwater H A. All-optical modulation by plasmonic excitation of CdSe quantum dots. Nature Photonics, 2007, 1(7): 402–406
11. Hu X, Jiang P, Ding C, Yang H, Gong Q. Picosecond and low-power all-optical switching based on an organic photonic-bandgap microcavity. Nature Photonics, 2008, 2(3): 185–189
12. Seibert K, Cho G C, Kütt W, Kurz H, Reitze D H, Dadap J I, Ahn H, Downer M C, Malvezzi A M. Femtosecond carrier dynamics in graphite. Physical Review B: Condensed Matter and Materials Physics, 1990, 42(5): 2842–2851
13. Breusing M, Ropers C, Elsaesser T. Ultrafast carrier dynamics in graphite. Physical Review Letters, 2009, 102(8): 086809-1–086809-4
14. Sun D, Wu Z K, Divin C, Li X, Berger C, de Heer W A, First P N, Norris T B. Ultrafast relaxation of excited Dirac fermions in epitaxial graphene using optical differential transmission spectroscopy. Physical Review Letters, 2008, 101(15): 157402-1–157402-4
15. Hendry E, Hale P J, Moger J, Savchenko A K, Mikhailov S A. Coherent nonlinear optical response of graphene. Physical Review Letters, 2010, 105(9): 097401-1–097401-4
16. Zhang H, Virally S, Bao Q, Ping L K, Massar S, Godbout N, Kockaert P. Z-scan measurement of the nonlinear refractive index of graphene. Optics Letters, 2012, 37(11): 1856–1858
17. Wu Y, Yao B, Cheng Y, Rao Y, Gong Y, Zhou X, Wu B, Chiang K S. Four-wave mixing in a microfiber attached onto a graphene film. IEEE Photonics Technology Letters, 2014, 26(3): 249–252
18. Wu Y, Yao B C, Feng Q Y, Cao X L, Zhou X Y, Rao Y J, Gong Y, Zhang W L, Wang Z G, Chen Y F, Chiang K S. Generation of cascaded four-wave-mixing with graphene-coated microfiber. Photonics Research, 2015, 3(2): A64–A68
19. Xia F, Mueller T, Lin Y M, Valdes-Garcia A, Avouris P. Ultrafast graphene photodetector. Nature Nanotechnology, 2009, 4(12): 839–843
20. Kim K, Choi J, Kim T, Cho S, Chung H. A role for graphen in silicon-based semiconductor devices. Nature, 2011, 479((7373)): 338–344
21. Liu M, Yin X, Zhang X. Double-layer graphene optical modulator. Nano Letters, 2012, 12(3): 1482–1485
22. Bao Q, Zhang H, Wang B, Ni Z, Lim C H Y X, Wang Y, Tang D Y, Loh K P. Broadband graphene polarizer. Nature Photonics, 2011, 5 (7): 411–415
23. Bao Q, Loh K P. Graphene photonics, plasmonics, and broadband optoelectronic devices. ACS Nano, 2012, 6(5): 3677–3694
24. Tong L, Lou J, Mazur E. Single-mode guiding properties of subwavelength-diameter silica and silicon wire waveguides. Optics Express, 2004, 12(6): 1025–1035
25. Tong L, Gattass R R, Ashcom J B, He S, Lou J, Shen M, Maxwell I, Mazur E. Subwavelength-diameter silica wires for low-loss optical wave guiding. Nature, 2003, 426(6968): 816–819
26. Brambilla G, Finazzi V, Richardson D J. Ultra-low-loss optical fiber nanotaper. Optics Express, 2004, 12(10): 2258–2263
27. Brambilla G, Xu F, Horak P, Jung Y, Koizumi F, Sessions N P, Koukharenko E, Feng X, Murugan G S, Wilkinson J S, Richardson D J. Optical fiber nanowires and microwires: fabrication and

applications. Advances in Optics and Photonics, 2009, 1(1): 107–161

28. Liu Z B, Feng M, Jiang W S, Xin W, Wang P, Sheng Q W, Liu Y G, Wang D N, Zhou W Y, Tian J G. Broadband all-optical modulation using a graphene-covered-microfiber. Laser Physics Letters, 2013, 10(6): 065901-1–065901-5
29. Li W, Chen B, Meng C, Fang W, Xiao Y, Li X, Hu Z, Xu Y, Tong L, Wang H, Liu W, Bao J, Shen Y R. Ultrafast all-optical graphene modulator. Nano Letters, 2014, 14(2): 955–959
30. Wu Y, Yao B, Cheng Y, Rao Y, Gong Y, Zhang W, Wang Z, Chen Y. Hybrid graphene-microfiber waveguide for chemical gas sensing. IEEE Journal of Selected Topics in Quantum Electronics, 2014, 20 (1): 4400206-1–4400206-6
31. Yao B, Wu Y, Cheng Y, Zhang A, Cong Y, Rao Y, Wang Z, Chen Y. All-optical Mach-Zehnder interferometric NH_3 gas sensor based on graphene/microfiber hybrid waveguide. Sensors and Actuators B: Chemical, 2014, 194: 142–148
32. Yao B C, Wu Y, Zhang A Q, Rao Y J, Wang Z G, Cheng Y, Gong Y, Zhang W L, Chen Y F, Chiang K S. Graphene enhanced evanescent field in microfiber multimode interferometer for highly sensitive gas sensing. Optics Express, 2014, 22(23): 28154–28162
33. Wu Y, Yao B, Zhang A, Rao Y, Wang Z, Cheng Y, Gong Y, Zhang W, Chen Y, Chiang K S. Graphene-coated microfiber Bragg grating for high-sensitivity gas sensing. Optics Letters, 2014, 39(5): 1235–1237
34. Sun Z, Hasan T, Torrisi F, Popa D, Privitera G, Wang F, Bonaccorso F, Basko D M, Ferrari A C. Graphene mode-locked ultrafast laser. ACS Nano, 2010, 4(2): 803–810
35. He X, Liu Z, Wang D, Yang M, Liao C R, Zhao X. Passively mode-locked fiber laser based on reduced graphene oxide on microfiber for ultra-wide-band doublet pulse generation. Journal of Lightwave Technology, 2012, 30(7): 984–989
36. Wang J, Luo Z, Zhou M, Ye C, Fu H, Cai Z, Cheng H, Xu H, Qi W. Evanescent-light deposition of graphene onto tapered fibers for passive *Q*-switch and mode-locker. IEEE Photonics Journal, 2012, 4 (5): 1295–1305
37. Sheng Q, Feng M, Xin W, Han T, Liu Y, Liu Z, Tian J. Actively manipulation of operation states in passively pulsed fiber lasers by using graphene saturable absorber on microfiber. Optics Express, 2013, 21(12): 14859–14866
38. Xin W, Liu Z B, Sheng Q W, Feng M, Huang L G, Wang P, Jiang W S, Xing F, Liu Y G, Tian J G. Flexible graphene saturable absorber on two-layer structure for tunable mode-locked soliton fiber laser. Optics Express, 2014, 22(9): 10239–10247
39. He X, Wang D N, Liu Z. Pulse-width tuning in a passively mode-locked fiber laser with graphene saturable absorber. IEEE Photonics Technology Letters, 2014, 26(4): 360–363
40. Luo Z Q, Wang J Z, Zhou M, Xu H Y, Cai Z P, Ye C Y. Multi-wavelength mode-locked erbium-doped fiber laser based on the interaction of graphene and fiber-taper evanescent field. Laser Physics Letters, 2012, 9(3): 229–233
41. Luo A, Zhu P, Liu H, Zheng X, Zhao N, Liu M, Cui H, Luo Z, Xu W. Microfiber-based, highly nonlinear graphene saturable absorber for formation of versatile structural soliton molecules in a fiber laser. Optics Express, 2014, 22(22): 27019–27025
42. Zhao N, Liu M, Liu H, Zheng X, Ning Q, Luo A, Luo Z, Xu W. Dual-wavelength rectangular pulse Yb-doped fiber laser using a microfiber-based graphene saturable absorber. Optics Express, 2014, 22(9): 10906–10913
43. Liu C, Ye C, Luo Z, Cheng H, Wu D, Zheng Y, Liu Z, Qu B. High-energy passively *Q*-switched 2 μm Tm^{3+}-doped double-clad fiber laser using graphene-oxide-deposited fiber taper. Optics Express, 2013, 21(1): 204–209
44. Sheng Q W, Feng M, Xin W, Guo H, Han T Y, Li Y G, Liu Y G, Gao F, Song F, Liu Z B, Tian J G. Tunable graphene saturable absorber with cross absorption modulation for mode-locking in fiber laser. Applied Physics Letters, 2014, 105(4): 041901-1–041901-5
45. Ren A, Feng M, Song F, Ren Y, Yang S, Yang Z, Li Y, Liu Z, Tian J. Actively *Q*-switched ytterbium-doped fiber laser by an all-optical *Q*-switcher based on graphene saturable absorber. Optics Express, 2015, 23(16): 21490–21496
46. Ahmad H, Dernaika M, Harun S W. All-fiber dual wavelength passive *Q*-switched fiber laser using a dispersion-decreasing taper fiber in a nonlinear loop mirror. Optics Express, 2014, 22(19): 22794–22801
47. Qi Y, Liu H, Cui H, Huang Q, Ning Q, Liu M, Luo Z, Luo A, Xu W, Graphene-deposited microfiber photonics device for ultrahigh-repetition rate pulse generation in a fiber laser. Optics Express, 2015, 23(14): 17720–17726
48. Bao Q, Zhang H, Wang Y, Ni Z, Yan Y, Shen Z X, Loh K P, Tang D Y. Atomic-layer graphene as a saturable absorber for ultrafast pulsed lasers. Advanced Functional Materials, 2009, 19(19): 3077–3083
49. Vakil A, Engheta N. Transformation optics using graphene. Science, 2011, 332(6035): 1291–1294
50. Yan S, Zheng B, Chen J, Xu F, Lu Y,Optical electrical current sensor utilizing a graphene-microfiber-integrated coil resonator. Applied Physics Letters, 2015, 107: 053502-1–053502-4
51. He X, Zhang X, Zhang H, Xu M. Graphene covered on microfiber exhibiting polarization and polarization-dependent saturable absorption. IEEE Journal of Selected Topics in Quantum Electronics, 2014, 20(1): 4500107-1–4500107-7
52. Sun X, Qiu C, Wu J, Zhou H, Pan T, Mao J, Yin X, Liu R, Gao W, Fang Z, Su Y. Broadband photodetection in a microfiber-graphene device. Optics Express, 2015, 23(19): 25209–25216
53. Xing X, Zheng J, Sun C, Li F, Zhu D, Lei L, Cai X, Wu T. Graphene oxide-deposited microfiber: a new photothermal device for various microbubble generation. Optics Express, 2013, 21(26): 31862–31871
54. Zhu B, Ren G, Gao Y, Yang Y, Lian Y, Jian S. Graphene-coated tapered nanowire infrared probe: a comparison with metal-coated probes. Optics Express, 2014, 22(20): 24096–24103

Xiaoying He received the B.S. degree in physics from Hubei Normal University. She received the M.S. and Ph.D. degrees from Huazhong University of Science and Technology, in 2006 and 2009, respectively.

From 2005 to 2006, she worked with Accelink Technology Company Ltd., Wuhan, China. From 2007 to 2008, she was a research assistant in The Hong Kong Polytechnic University. From 2009 to 2011, she worked as a Post-doctor

Research Fellow at The Hong Kong Polytechnic University. She had joined Fudan University in 2012 as a Lecture of Department of Optical Science and Technology. In 2015, she worked as an associate professor in Fudan University. Her main research interests are semiconductor optoelectronic devices, fiber laser, optical fiber sensors and optical design.